Molecular and Cellular Neuroscience 88 (2018) 138–147

Contents lists available at ScienceDirect

Molecular and Cellular Neuroscience

journal homepage: www.elsevier.com/locate/ymcne

G-protein coupled receptors Mc4r and Drd1a can serve as surrogate odorant receptors in mouse olfactory sensory neurons

Markella Katidou[a], Xavier Grosmaitre[b], Jiangwei Lin[a], Peter Mombaerts[a,*]

[a] Max Planck Research Unit for Neurogenetics, Frankfurt, Germany
[b] Centre des Sciences du Goût et de l'Alimentation, AgroSup Dijon, CNRS, INRA, Université Bourgogne Franche-Comté, F-21000 Dijon, France

ARTICLE INFO

Keywords:
Main olfactory epithelium
Glomerulus
Odorant receptor
G-protein coupled receptor
Dopamine
Melanocortin

ABSTRACT

In the mouse, most mature olfactory sensory neurons (OSNs) express one allele of one gene from the repertoire of ~1100 odorant receptor (OR) genes, which encode G-protein coupled receptors (GPCRs). Axons of OSNs that express a given OR coalesce into homogeneous glomeruli, which reside at conserved positions in the olfactory bulb. ORs are intimately involved in ensuring the expression of one OR per OSN and the coalescence of OSN axons into glomeruli. But the mechanisms whereby ORs accomplish these diverse functions remain poorly understood. An experimental approach that has been informative is to substitute an OR genetically with another GPCR that is normally not expressed in OSNs, in order to determine in which aspects this GPCR can serve as surrogate OR in mouse OSNs. Thus far only the β2-adrenergic receptor (β2AR, Ardb2) has been shown to be able to serve as surrogate OR in OSNs; the β2AR could substitute for the M71 OR in all aspects examined. Can other non-olfactory GPCRs function equally well as surrogate ORs in OSNs? Here, we have generated and characterized two novel gene-targeted mouse strains in which the mouse melanocortin 4 receptor (Mc4r) or the mouse dopamine receptor D1 (Drd1a) is coexpressed with tauGFP in OSNs that express the OR locus *M71*. These alleles and strains are abbreviated as Mc4r → M71-GFP and Drd1a → M71-GFP. We detected strong Mc4r or Drd1a immunoreactivity in axons and dendritic knobs and cilia of OSNs that express Mc4r or Drd1a from the *M71* locus. These OSNs responded physiologically to cognate agonists for Mc4r (Ro27-3225) or Drd1a (SKF81297), and not to the M71 ligand acetophenone. Axons of OSNs expressing Mc4r → M71-GFP coalesced into glomeruli. Axons of OSNs expressing Drd1a → M71-GFP converged onto restricted areas of the olfactory bulb but did not coalesce into glomeruli. Thus, OR functions in OSNs can be substituted by Mc4r or Drd1a, but not as well as by β2AR. We attribute the weak performance of Drd1a as surrogate OR to poor OSN maturation.

1. Introduction

Most mature OSNs express one allele of one of the ~1100 OR genes (Buck and Axel, 1991) in the mouse genome (Chess et al., 1994; Malnic et al., 1999; Strotmann et al., 2000). Axons from OSNs that express the same OR coalesce into one or a few homogeneous glomeruli in the medial and lateral halves of the olfactory bulb (Mombaerts et al., 1996). These OR-specific glomeruli reside at conserved but not stereotyped positions (Zapiec and Mombaerts, 2015) within the array of ~3600 glomeruli in the olfactory bulb of an adult mouse (Richard et al., 2010). Within these glomeruli OSN axons make synaptic contact with interneurons and second-order neurons in the olfactory pathway. The expressed OR is intimately involved in the process of axonal coalescence (Mombaerts et al., 1996).

It remains poorly understood how ORs exercise such widely diverse functions in the molecular and cellular mechanisms of OR gene choice and OSN axonal coalescence into glomeruli. A first question that comes to mind is whether these functional properties are specific to ORs, or whether other GPCRs can substitute, partially or fully, for ORs in OSNs under experimental conditions. Of particular interest are the non-olfactory GPCRs that can couple to G_{α}olf (Gnal) or G_{α}s (Gnas), the G protein subunits to which ORs couple within OSNs (Jones and Reed, 1989; Belluscio et al., 1998). We have shown that the mouse β2-adrenergic receptor (Ardb2, abbreviated β2AR) can serve as surrogate OR in OSNs when expressed from the *M71* locus by gene targeting (Feinstein et al., 2004; Omura et al., 2014). In independent studies, β2AR

Abbreviations: β2AR, β2-adrenergic receptor; Drd1a, dopamine receptor D1; IHC, immunohistochemistry; IRES, internal ribosome entry site; ISH, in situ hybridization; GFP, green fluorescent protein; GPCR, G-protein coupled receptor; Mc4r, melanocortin 4 receptor; MOE, main olfactory epithelium; NGS, normal goat serum; OR, odorant receptor; OSN, olfactory sensory neuron; PBS, phosphate-buffered saline; PD, postnatal day; PFA, paraformaldehyde

* Corresponding author at: Max Planck Research Unit of Neurogenetics, Max-von-Laue-Strasse 4, D-60438 Frankfurt, Germany.
E-mail address: peter.mombaerts@gen.mpg.de (P. Mombaerts).

https://doi.org/10.1016/j.mcn.2018.01.010
Received 9 November 2017; Received in revised form 26 January 2018; Accepted 29 January 2018
Available online 31 January 2018

expression driven from a MOR23 transgene (Vassalli et al., 2002) also resulted in OSN axonal coalescence into glomeruli (Aoki et al., 2013; Nakashima et al., 2013). It remains to be seen if other non-olfactory GPCRs that can couple to Gnal or Gnas and that are normally not expressed in OSNs can serve equally well as surrogate ORs when expressed from an endogenous OR locus.

Here, we set out to test if and to which extent mouse Mc4r and Drd1a can substitute for an OR in OSNs when expressed from the *M71* locus by gene targeting.

2. Materials and methods

2.1. Gene targeting

To create the Mc4r → M71-IRES-tauGFP and Drd1a → M71-IRES-tauGFP gene-targeted mutations, we replaced the coding sequence of *M71* with the coding sequence of mouse *Mc4r* and *Drd1a*, respectively, using a generic M71 targeting vector that we described previously (Feinstein et al., 2004; Omura et al., 2014). By gene synthesis (GeneArt), we constructed DNA fragments that include part of the M71 promoter (187 bp from the single *StuI* site to the *ATG* start codon in the M71 targeting vector of Feinstein et al., 2004), followed by the coding sequence of mouse *Mc4r* (accession NM_016977.4) or mouse *Drd1a* (accession MN_010076.3), a *TGT* codon after the stop codon, and *AscI* and *PacI* restriction sites. The length of these synthetic DNA fragments was 1206 and 1548 bp, respectively. The synthetic fragments were then cloned into the *M71* targeting vector at the *StuI/PacI* sites. Finally the *IRES-tauGFP-ACNF* cassette was cloned into the *AscI* site. The *ACNF* cassette contains a neomycin selectable marker gene that is self-excised by Cre-mediated recombination in the male germline, leaving a single *loxP* site behind. The Mc4r → M71-IRES-tauGFP and Drd1a → M71-IRES-tauGFP targeting vectors are publicly available from Addgene as #105072 and #105073, respectively. Gene targeting was carried out in the parental ES cell line E14 by electroporation as described (Mombaerts et al., 1996). Genomic DNA from G418-resistant ES clones was screened for homologous recombination by non-radioactive Southern blot hybridization using a probe that is external to the targeting vector. ES cells from gene-targeted clones were injected into C57BL/6 J blastocysts, and male chimeras were crossed with C57BL/6 J females. Germline transmission was obtained with clones B179 and A25, respectively. The Mc4r → M71-IRES-tauGFP and Drd1a → M71-IRES-tauGFP strains were established and maintained in a mixed 129P2/OlaHsd x C57BL/6J background, and are abbreviated Mc4r → M71-GFP and Drd1a → M71-GFP. The strains are publicly available from The Jackson Laboratory: Mc4r → M71-GFP as stock #28199 and official strain name B6;129P2-Olfr151 < tm42(Mc4r)Mom > /MomJ, and Drd1a → M71-GFP as stock #27251 and official strain name B6;129P2-Olfr151 < tm41(Drd1a)Mom > /MomJ. The MOE was analyzed at postnatal day (PD) 21, and the olfactory bulb at PD10 unless indicated otherwise. Mouse experiments comply with the ARRIVE guidelines, and were performed in accordance with the German Animal Welfare Act, the European Communities Council Directive 2010/63/EU, and the institutional ethical and animal welfare guidelines of the Max Planck Research Unit for Neurogenetics.

2.2. In situ hybridization

Three-color in situ hybridization (ISH) was performed as previously described (Ishii et al., 2004). *GFP* + cells were visualized with a mixture of *tau* and *GFP* probes, and *Omp* and *Gap43* probes were used to characterize the maturation state of the cells (Ishii et al., 2004).

2.3. Immunohistochemistry

Mice were anaesthetized by injection of ketamine HCl and xylazine at 150 mg/kg and 10 mg/kg body weight, respectively. They were then perfused with ice-cold PBS, followed by 4% PFA in PBS. The mouse heads were dissected, and post-fixed in 4% PFA for 2 h. The nose was decalcified in 0.45 M EDTA in 1× PBS overnight at 4 °C. Next the samples were incubated in 15% and 30% sucrose in 1× PBS overnight at 4 °C, embedded and frozen in O.C.T. compound, and sectioned at 12 or 16 µm with a Leica CM3500 cryostat. Sections were permeabilized with 0.5% Triton X-100 in 1× PBS, and blocked with 10% NGS, 0.5% Triton X-100 in 1× PBS for 1 h at room temperature. After the blocking step, sections were incubated in 10% NGS, 0.5% Triton X-100 in 1× PBS overnight at 4 °C with rat monoclonal anti-Drd1a (1:1000, Sigma #D2944), rabbit polyclonal anti-Mc4r (1:100, Alomone labs #AMR-024), mouse monoclonal anti-MAP2 (1:500, Sigma #M9942), guinea pig polyclonal anti-VGLUT2 (1:1000, Synaptic Systems #135404), and chicken polyclonal anti-GFP (1:1000, Abcam #13970). After incubation with primary antibodies and washes, sections were incubated with blocking solution for 1 h at room temperature, followed by incubation with secondary antibodies for 2 h at room temperature: Alexa 546-conjugated goat anti-rat IgG (1:500, Thermo Fisher Scientific #A-11081), Alexa 546-conjugated goat anti-rabbit IgG (1:500, Thermo Fisher Scientific #A-11035), Alexa 647-conjugated goat anti-mouse (1:500, Thermo Fisher Scientific #A28181), RRX goat anti-guinea pig IgG (Jackson ImmunoResearch Laboratories #106-295-006), Alexa 488-conjugated goat anti-chicken IgY (1:500, Thermo Fisher Scientific #A-11039). Olfactory bulb sections were counterstained with 0.1 µg/ml DAPI (1:10,000, Thermo Fisher Scientific #D1306). Sections were analyzed with a Zeiss LSM 710 confocal microscope.

2.4. Wholemount immunohistochemistry

Wholemount immunohistochemistry (IHC) was performed as described (Dietschi et al., 2013; Strotmann et al., 2004). Briefly, we dissected olfactory turbinates from PD21 mice. The wholemounts were fixed in MeOH for 20 min at −20 °C, washed with 0.5% TritonX-100 in 1× PBS, and blocked with 10% NGS, 0.5% TritonX-100 in 1× PBS for 1 h at room temperature with gentle agitation. Incubation with primary antibodies was performed as with the sections. After washing with 0.5% TritonX-100 in 1× PBS, wholemounts were incubated with blocking solution for 1 h, followed by Alexa 546-conjugated goat anti-rabbit or rat IgG (1:500, Thermo Fisher Scientific #A-11081 and #A-11035, respectively) in 1× PBS containing 10% NGS, 0.5% TritonX-100 for 2 h at room temperature. After washing with 0.5% TritonX-100 in 1× PBS, stained samples were kept in 1× PBS, and images of samples were collected with a Zeiss LSM 710 confocal microscope. For STED preparations secondary antibodies were goat anti-rat STAR RED (1:200, Abberior #2-0132-011-2) and goat anti-rabbit 635P (1:200, Abberior #2-0012-007-2). Samples were mounted with liquid mounting medium (Abberior #4-0100-005-0) and visualized with a custom-built STED super-resolution microscope (Abberior Instruments) that is based on a Zeiss LSM 510 confocal microscope.

2.5. Cell counts in the MOE and glomerular volume

To estimate the total number of OSNs that express a mutant allele, we followed a method that we described previously (Bressel et al., 2016). Briefly, we made 12 µm cryosections and counted OSNs that display the intrinsic green fluorescence in every fifth coronal section. We applied an Abercrombie correction factor of 0.74 that we calculated for OSNs that express the *M71* locus (Bressel et al., 2016). We estimated the glomerular volume for each 12 µm section as previously described (Bressel et al., 2016).

2.6. Patch-clamp recordings

Mice were anaesthetized by injection of ketamine HCl and xylazine, and then decapitated. The head was immediately put into ice-cold Ringer's solution, which contained (in mM): NaCl 124, KCl 3, $MgSO_4$

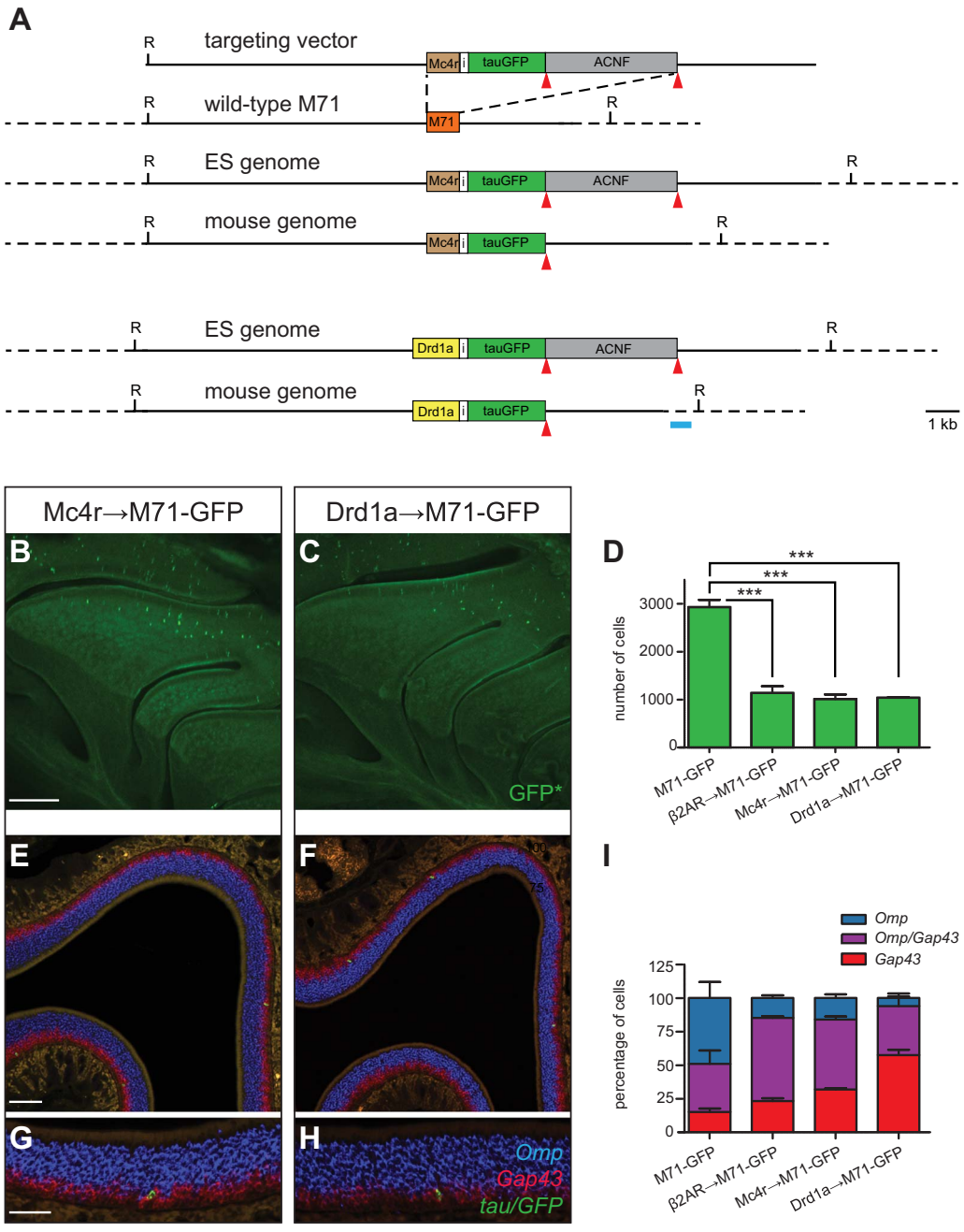

Fig. 1. The mouse strains Mc4r → M71-IRES-tauGFP and Drd1a → M71-IRES-tauGFP.
(A) Replacement of the coding sequence of *M71* by the coding sequence of *Mc4r* or *Drd1a* by gene targeting in ES cells. The upper schematic shows the Mc4r → M71-GFP targeting vector, the wild-type *M71* locus, and the Mc4r → M71-GFP allele before (ES genome) and after (mouse genome) self-excision of the *ACNF* cassette. This cassette comprises a neo selectable marker gene that is removed during transmission through the male germ line, leaving a single *loxP* site (red triangle) behind in the mouse genome. The lower schematic shows the Drd1a → M71-GFP allele before and after self-excision of the *ACNF* cassette. The horizontal turquoise bar represents the external probe for the screening of homologous recombination by Southern blot hybridization of genomic DNA of ES clones. Dashed lines represent genomic sequences 5′ and 3′ to the targeting vector.
(B, C) Intrinsic green fluorescence of GFP (GFP*) in wholemount medial views of the MOE on the turbinates of Mc4r → M71-GFP and Drd1a → M71-GFP mice at PD21. Left is anterior, top is dorsal.
(D) The number of OSNs per mouse that display intrinsic green fluorescence of GFP in the strains β2AR → M71-GFP, Mc4r → M71-GFP and Drd1a → M71-GFP compared with the M71-GFP strain.
(E–H) Three-color ISH of coronal cryosections of the MOE of Mc4r → M71-GFP and Drd1a → M71-GFP mice at PD21 with riboprobes for *Omp* (blue), *Gap43* (red), and *tau/GFP* (green). High magnifications show *GFP*+ cells that are *Omp*- *Gap43*+ (G,H).
(I) Percentages of OSNs that are *Omp* + *Gap43*- (blue), *Omp* + *Gap43*+ (magenta), or *Omp*- *Gap43*+ (red) by three-color ISH in PD21 mice of the strains M71-GFP, β2AR → M71-GFP, Mc4r → M71-GFP, and Drd1a → M71-GFP.
Scale bars: in B for B and C, 500 µm; in E for E and F, 100 µm; in G for G and H, 50 µm. (For interpretation of the references to color in this figure legend, the reader is referred to the web version of this article.)

1.3, $CaCl_2$ 2, $NaHCO_3$ 26, NaH_2PO_4 1.25, glucose 15; pH 7.6 and 305 mOsm. The pH was kept at 7.4 by bubbling with 95% O_2 and 5% CO_2. The nose was dissected out en bloc. The MOE attached to the nasal septum and the dorsal recess was removed and kept in oxygenated Ringer. Immediately before starting the recording session, the entire MOE was peeled away from the underlying bone and transferred to a recording chamber with the mucus layer facing up. Oxygenated Ringer was continuously perfused at room temperature.

The dendritic knobs of OSNs were visualized with an upright microscope (Olympus BX51WI) equipped with an Olympus DP72 camera and a 40× water-immersion objective. An extra 2× magnification was obtained by a magnifying lens in the light path. GFP + OSNs were visualized under fluorescent illumination. Superimposition of the fluorescent and bright-field images allowed identification of the fluorescent cells under bright field, which directed the recording pipettes. Electrophysiological recordings were controlled by an EPC-10 USB amplifier and with Patchmaster software (HEKA Electronic, Germany). Perforated patch clamp was performed on the dendritic knobs by including 260 µM nystatin in the recording pipette, which was filled with the following solution (in mM): KCl 70, KOH 53, methanesulfonic acid 30, EGTA 5, HEPES 10, sucrose 70; pH 7.2 (KOH) and 310 mOsm. The junction potential was ~9 mV and was corrected in all experiments offline. Under voltage-clamp mode, the signals were filtered at 10 kHz followed by 2.9 kHz, and sampled at 20 kHz.

A seven-barrel pipette was used to deliver stimuli by pressure ejection through a picospritzer (Pressure System IIe, Toohey Company, Fairfield, NJ). The stimulus electrode was placed ~20 µm downstream from the recording site. Distance and pressure were adjusted in order to minimize mechanical responses (Grosmaitre et al., 2006). Stimuli were delivered at a 138 kPa (~20 psi) pressure indicated on the picospritzer, with a 500 ms pulse length. Stock solutions of Ro27-3225 trifluoroacetate salt (Sigma #R3905; 2 mM in water), and SKF81297 hydrobromide (Tocris #1447, 100 mM in DMSO), were prepared and stored at −20 °C until use; the final solutions were prepared before

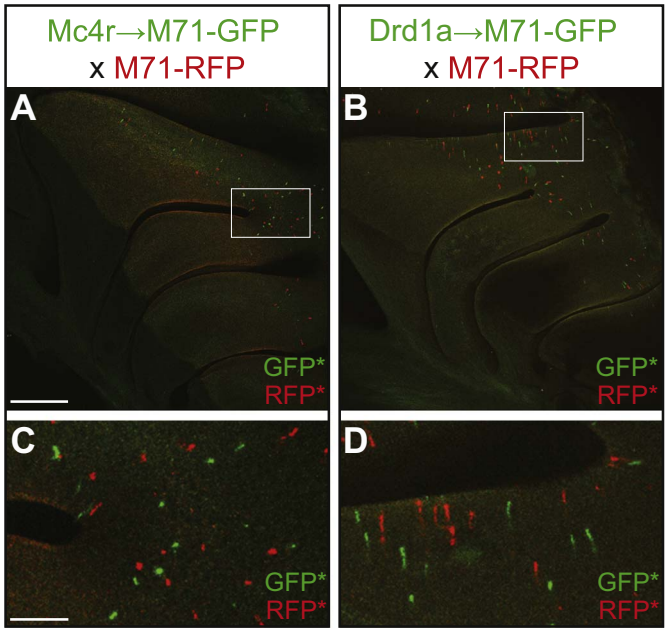

Fig. 2. Monoallelic expression of Mc4r → M71-GFP and Drd1a → M71-GFP.
(A, B) Wholemount medial views of the MOE on the turbinates of double heterozygous Mc4r → M71-GFP × M71-RFP mice (A) and Drd1a → M71-GFP × M71-RFP mice (B) at PD21. Intrinsic green (GFP*) and red (RFP*) fluorescence is mutually exclusive across OSNs, reflecting monoallelic expression at the *M71* locus.
(C–D) Enlarged representations of the areas in rectangles in A and B.
Scale bars: in A for A and B, 500 µm; in C for C and D, 125 µm. (For interpretation of the references to color in this figure legend, the reader is referred to the web version of this article.)

each experiment by adding Ringer. The odorant mixture consists of 19 compounds in equal molar concentration (Grosmaitre et al., 2009; Tazir et al., 2016): heptanol, octanol, hexanal, heptanal, octanal, heptanoic acid, octanoic acid, cineole, amyl acetate, (+) limonene, (−) limonene, (+) carvone, (−) carvone, 2-heptanone, anisaldehyde, benzaldehyde, acetophenone, 3-heptanone, and ethyl vanillin. Odorant mixture was prepared as a 0.1 M solution in DMSO and kept at −20 °C; final solutions at 10^{-5} M for each odorant were prepared before each experiment by adding Ringer. Forskolin, an activator of adenylyl cyclase, was prepared as a 10 mM stock solution in DMSO. IBMX, an inhibitor of phosphodiesterases, was prepared as a 100 mM stock solution in DMSO. Final solutions containing 200 µM of IBMX and 20 µM of forskolin were prepared before each experiment by adding Ringer. All chemicals were obtained from Sigma-Aldrich unless otherwise stated. Data were analyzed using Fitmaster (HEKA). Maximum amplitude of the response and kinetics characteristics were measured.

In these recording conditions, only OSNs that fit certain criteria can be recorded: the OSN must have a dendritic knob that is standing out from the surface of the preparation and is therefore available to be reached by the electrode. Such OSNs happen to bear cilia. As a consequence, all recorded OSNs can be considered as mature. In both strains, the number of OSNs fitting these criteria was low: ~20 for each ex vivo preparation, depending on the age and the success of the dissection.

3. Results

3.1. Expression of Mc4r and Drd1a from the M71 locus in OSNs

We generated two novel gene-targeted mouse strains in which the coding sequence of the *M71* OR was replaced by the coding sequence of two non-olfactory mouse GPCRs, *Mc4r* and *Drd1a*. The choice of these GPCRs was based on the following criteria: absence of expression in the MOE, a single coding exon, binding to Gnas, and commercial availability of agonists. Mc4r shares 14% amino acid identity with M71, and binds Gnas (Gantz et al., 1993) and other G_α proteins (Tao, 2010). Drd1a shares 16% amino acid identity with M71, and its coupling to adenylate cyclase is mediated by Gnas (Beaulieu and Gainetdinov, 2011) and Gnal (Zhuang et al., 2000). The design and generation of the Mc4r → M71-GFP and Drd1a → M71-GFP mutations (Fig. 1A) is according to what we reported previously for β2AR → M71-IRES-taulacZ (Feinstein et al., 2004) and for β2AR → M71-IRES-tauGFP (abbreviated β2AR → M71-GFP, Omura et al., 2014).

In wholemount medial views of the MOE on the turbinates, scattered OSNs displaying intrinsic green fluorescence of GFP were detected in a dorsal region of the MOE of Mc4r → M71-GFP and Drd1a → M71-GFP mice (Fig. 1B, C). To estimate the total number of GFP+ OSNs per mouse, we made coronal cryosections of the MOE of M71-GFP, β2AR → M71-GFP, Mc4r → M71-GFP, and Drd1a → M71-GFP mice at PD21 (n = 3 per strain), and counted labeled cells using a method that we described previously (Bressel et al., 2016). Our estimates are 2928 ± 152 (mean ± STDV) GFP+ OSNs in M71-GFP mice, 1139 ± 138 in β2AR → M71-GFP mice, 1013 ± 92 in Mc4r → M71-GFP mice, and 1038 ± 14 in Drd1a → M71-GFP mice (Fig. 1D). Thus, the number of GFP+ OSNs is reduced by a factor of three-fold in these three strains compared to M71-GFP mice (1-way ANOVA, $p < 0.001$).

To characterize the maturation state of OSNs, we performed three-color in situ hybridization (ISH) with riboprobes for *Omp* (mature cells), *Gap43* (immature cells), and a mix for *tau* and *GFP* (Fig. 1E–H). We counted 107, 262, 85 and 80 *GFP*+ OSNs in M71-GFP, β2AR → M71-GFP, Mc4r → M71-GFP, and Drd1a → M71-GFP mice respectively. We found that 32% and 58% of *GFP*+ OSNs in Mc4r → M71-GFP mice and Drd1a → M71-GFP mice respectively are *Omp- Gap43*+ (and are thus immature), compared to 15% in M71-GFP mice ($p > 0.05$ and $p < 0.001$, respectively, 2-way ANOVA) (Fig. 1I). In β2AR → M71-GFP mice, this fraction is 23%, which is significantly lower compared to Drd1a → M71-GFP mice ($p < 0.001$, 2-way ANOVA). The fraction of *GFP*+ cells that is *Omp* + *Gap43*- (and are thus mature) is 49% for M71-GFP, 15% for β2AR → M71-GFP, 16% for Mc4r → M71-GFP, and 6% for Drd1a → M71-GFP mice ($p < 0.001$ for all in comparison with M71-GFP, 2-way ANOVA). Thus, the fraction of immature cells is increased and the fraction of mature cells is decreased in Mc4r → M71-GFP and Drd1a → M71-GFP mice compared to M71-GFP mice and β2AR → M71-GFP mice.

3.2. Monoallelic expression of Mc4r and Drd1a from the M71 locus in OSNs

To determine whether expression of the Mc4r → M71-GFP and Drd1a → M71-GFP alleles is monoallelic, we crossed Mc4r → M71-GFP mice and Drd1a → M71-GFP mice with M71-IRES-tauRFP mice (abbreviated M71-RFP, Li et al., 2004; Omura et al., 2014). In wholemounts of the MOE on the turbinates of Mc4r → M71-GFP × M71-RFP double heterozygous mice at PD21 (n = 7), we counted 288 GFP+ and 314 RFP+ cells, and did not observe OSNs that displayed both intrinsic green and red fluorescence (Fig. 2A,C). In Drd1a → M71-GFP × M71-RFP double heterozygous mice at PD21 (n = 4), we counted 122 GFP+ and 141 RFP+ OSNs, but did not observe OSNs that displayed both intrinsic green and red fluorescence (Fig. 2B, D). These data are consistent with monoallelic expression of *Mc4r* and *Drd1a* expression from the *M71* locus.

3.3. Mc4r and Drd1a proteins are expressed in dendritic knobs and cilia

Next, we examined whether Mc4r and Drd1a protein expression resembles the typical OR subcellular expression pattern spanning the cell body, dendrite, dendritic cilia, and axons of OSNs (Barnea et al., 2004; Feinstein et al., 2004; Strotmann et al., 2004) (Fig. 3). In coronal sections of the MOE of Mc4r → M71-GFP and Drd1a → M71-GFP mice

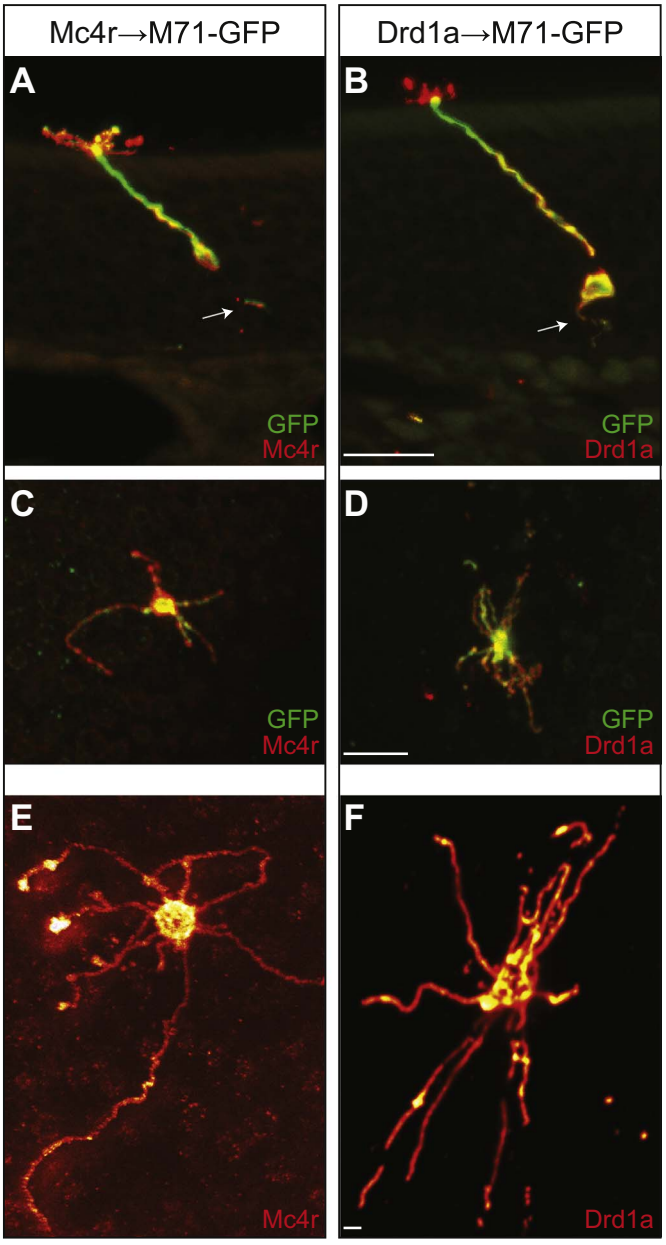

Fig. 3. Mc4r and Drd1a immunoreactivity in OSN cell bodies, axons, dendrites, and cilia of Mc4r → M71-GFP and Drd1a → M71-GFP mice.

(A, B) Confocal imaging of immunoreactivity for GFP (green) and Mc4r (A) or Drd1a (B) (red) in coronal cryosections of the MOE of Mc4r → M71-GFP and Drd1a → M71-GFP mice at PD21. The arrows indicate traces of OSN axons stained with antibodies against Mc4r or Drd1a and GFP. The overlay of red and green signal is yellow.

(C, D) Confocal *en face* imaging of wholemounts of MOE of Mc4r → M71-GFP and Drd1a → M71-GFP mice at PD21 reveals dense immunoreactive signal for Mc4r (C) and Drd1a (D) in the dendritic knob and cilia of an individual OSN at PD21.

(E, F) STED super-resolution *en face* imaging of wholemounts of MOE of Mc4r → M71-GFP and Drd1a → M71-GFP mice at PD21 reveals dense immunoreactive signal for Mc4r (E) and Drd1a (F) throughout the dendritic knob and cilia. A stronger signal for Mc4r and Drd1a is present in the dendritic knob and in the endings of cilia.

Scale bars: in B for A and B, 25 µm; in D for C and D, 10 µm; in F for E and F, 1 µm. (For interpretation of the references to color in this figure legend, the reader is referred to the web version of this article.)

at PD21, we found that Mc4r or Drd1a immunoreactivity colocalizes with GFP immunoreactivity in cell bodies and dendrites of OSNs (Fig. 3A, B). *En face* view of wholemounts of the MOE revealed dense immunoreactive signal of Mc4r and Drd1a in the dendritic knob and cilia of OSNs (Fig. 3C, D). As expected, we did not observe Mc4r or Drd1a immunoreactivity in GFP- cells. Finally we used STED super-resolution microscopy to visualize better the expression of Mc4r and Drd1a protein in the cilia. The Mc4r immunoreactive signal appears highly concentrated in the dendritic knob and endings of the cilia (Fig. 3E). The Drd1a immunoreactive signal appears more equally distributed in the cilia compared to that of Mc4r (Fig. 3F). Mc4r → M71-GFP OSNs possess 8.1 ± 1.5 cilia (n = 14), and Drd1a → M71-GFP OSNs have 10.2 ± 1.3 cilia (n = 7) (± STDV, $p < 0.05$, Student's *t*-test). Taken together, the subcellular pattern of Mc4r and Drd1a immunoreactivity resembles that of ORs, thus fulfilling a prerequisite for these non-olfactory ORs to serve as surrogate ORs in terms of signal transduction.

3.4. Mc4r and Drd1a-expressing OSNs respond to their cognate agonists

Next, we examined the membrane properties of Mc4r and Drd1a-expressing OSNs by perforated patch-clamp electrophysiology on the dendritic knob of OSNs in an intact preparation, as described previously (Ma et al., 1999; Grosmaitre et al., 2006; Grosmaitre et al., 2009; Lam and Mombaerts, 2013; Omura et al., 2014; Tazir et al., 2016).

We tested Ro27-3225 as a selective agonist for Mc4r (Agosti et al., 2014; Benoit et al., 2000; Giuliani et al., 2007) (Fig. 4). Representative examples of traces of recordings from GFP + OSNs are shown in Fig. 4A. We recorded the response of five GFP + OSNs from Mc4r → M71-GFP mice between PD10 and PD15 to Ro27-3225 concentrations ranging from 10^{-7} to 10^{-4} M. We found that all five cells responded to 10^{-4} and 10^{-5} M of Ro27-3225, and that no OSN responded to 10^{-6} or 10^{-7} M (Fig. 4A). To confirm that the M71 OR is not expressed in these cells, we stimulated five GFP + OSNs with 10^{-5} M acetophenone, a ligand for M71 OR (Bozza et al., 2002), and found that none of these cells responded. To exclude expression of other, unidentified OR(s), we stimulated five GFP + OSNs with a mixture of 19 odorants that elicits a response in > 60% of randomly patched OSNs (Omura et al., 2014), and found that none of these OSNs responded. To examine the transduction pathway capacity, we stimulated five GFP + OSNs with a mixture of IBMX and forskolin, which are general activators of the signal transduction pathway in OSNs, and found that all cells responded. To confirm that Mc4r is not expressed in OSNs, we recorded from 10 randomly chosen GFP- OSNs from the same mice, and found none of the cells responded to Ro27–3225, even at concentrations of 10^{-5} and 10^{-4} M. Four out of 10 GFP- OSNs responded to 10^{-5} M of the odorant mixture, and 10 out of 10 GFP- OSNs responded to IBMX and forskolin. Examples of traces of recordings from GFP- OSNs are shown in Fig. 4B. Thus, Mc4r → M71-GFP OSNs responded to the selective Mc4r agonist Ro27-3225, and did not appear to express M71 or other ORs.

We tested SKF81297 as a selective agonist for Drd1a (Neumeyer et al., 2003; Rashid et al., 2007) (Fig. 5). Representative examples of traces of recordings from GFP + OSNs are shown in Fig. 5A. We recorded the response of six GFP + OSNs from Drd1a → M71-GFP mice between PD7 to PD10 to SKF81297 concentrations ranging from 10^{-7} to 10^{-4} M. We found that all cells responded to 10^{-4} and 10^{-5} M, two to 10^{-6} M, and none to 10^{-7} M. We also recorded responses from seven GFP + OSNs to lower concentrations (10^{-10} M to 10^{-7} M), and observed no response (data not shown). To confirm that the M71 OR is not expressed in these cells, we also stimulated 13 GFP + neurons with 10^{-5} M acetophenone, and found that none of the cells responded. None of the 13 GFP + OSNs responded to the odorant mixture. All 13 GFP + OSNs responded to IBMX and forskolin, indicating the presence and activity of a cAMP transduction pathway machinery. To confirm that Drd1a is not expressed in randomly chosen GFP- OSNs, we recorded from 10 GFP- OSNs from the same mice, and found that none of cells responded to SKF81297, even at the highest concentrations (10^{-5} and 10^{-4} M). Six out of 10 GFP- OSNs responded to 10^{-5} M of the odorant mixture, and 10 out of 10 GFP- OSNs responded to IBMX and forskolin. Representative examples of traces of recordings from GFP- OSNs are shown in Fig. 5B. Thus, Drd1a → M71-GFP OSNs responded to

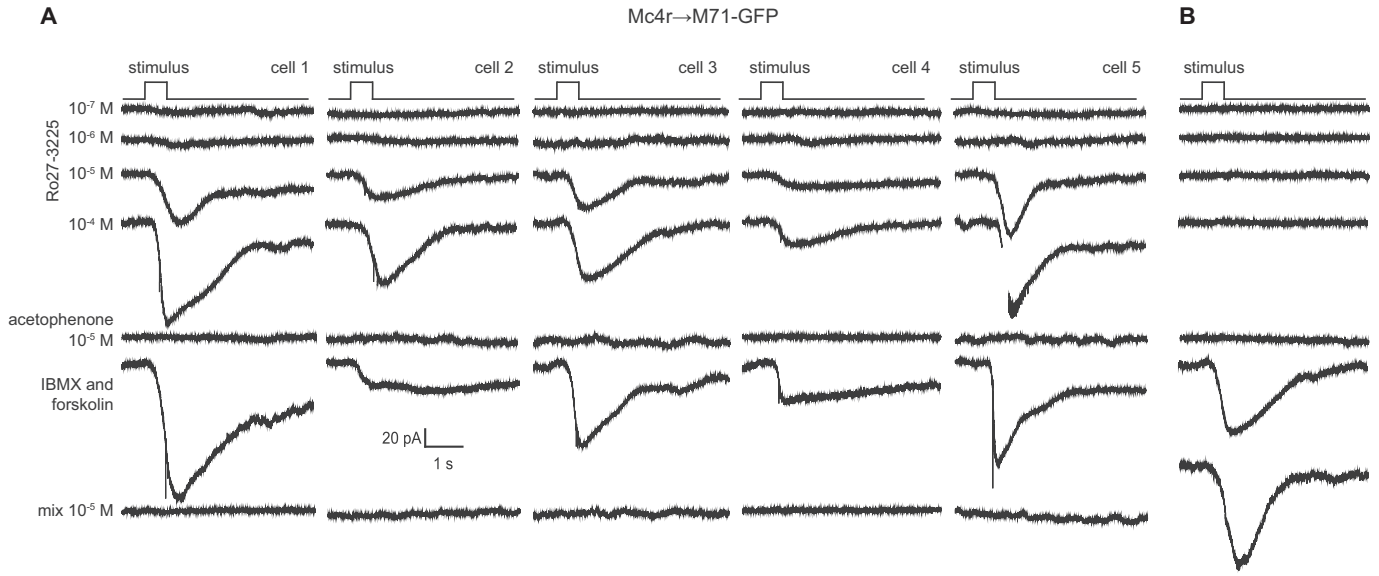

Fig. 4. OSNs expressing Mc4r → M71-GFP respond physiologically to Mc4r agonist Ro27–3225.
(A) Ro27-3225-induced inward currents in five GFP + cells from homozygous Mc4r → M71-GFP mice between PD10 to PD15. These cells also responded to IBMX and forskolin, but not to the M71 ligand acetophenone, and not to the odorant mixture.
(B) A randomly picked GFP- cell from the same mouse as cell 1 in (A) did not respond to Ro27-3225 and to acetophenone, but responded to IBMX and forskolin, and to the odorant mixture.

the selective agonist SKF81297, and did not appear to express M71 or other ORs.

3.5. Axons of Mc4r or Drd1a-expressing OSNs project to positions anterior to M71 glomeruli

We addressed whether Mc4r and Drd1a-expressing OSN axons form glomeruli (Fig. 6). By examing wholemounts of the olfactory bulbs in a confocal microscope at PD21, we found weak or no intrinsic green fluorescence in Mc4r → M71-GFP and Drd1a → M71-GFP mice. We thus shifted our analysis to younger mice, at PD7 and PD10. In M71-GFP mice at PD7, OSN axons coalesced at posterior-dorsal positions, and had started to form glomeruli (Fig. 6A). In β2AR → M71-GFP mice at PD7, OSN axons coalesced at more anterior-ventral positions (Fig. 6B) in comparison with labeled glomeruli in M71-GFP mice (Feinstein et al., 2004; Omura et al., 2014). In Mc4r → M71-GFP mice at PD7, OSN

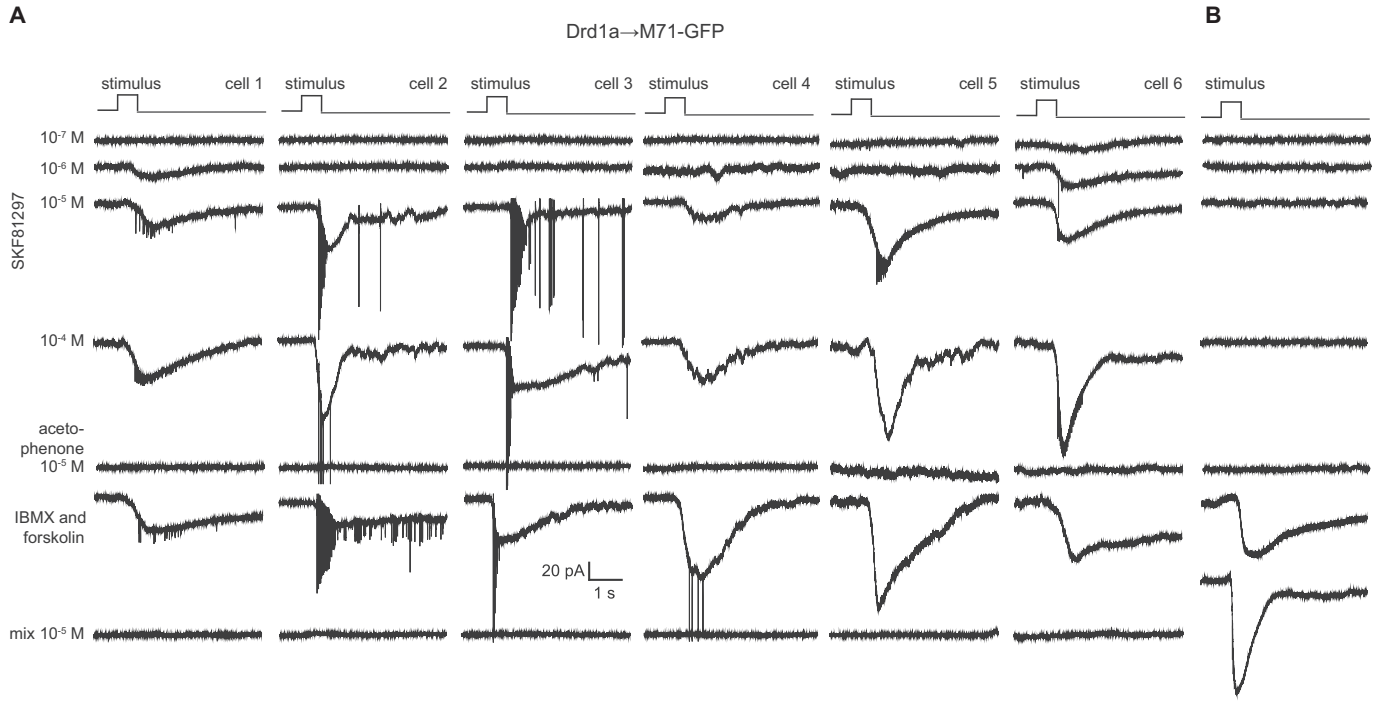

Fig. 5. OSNs expressing Drd1a → M71-GFP respond physiologically to Drd1a agonist SKF81297.
(A) SKF81297-induced inward currents in six GFP + cells from homozygous Drd1a → M71-GFP mice between PD7 to PD10. These cells also responded to IBMX and forskolin, but not to acetophenone, and not to the odorant mixture.
(B) A randomly picked GFP- cell from a homozygous Drd1a → M71-GFP mouse did not respond to SKF81297 and to acetophenone, but responded to IBMX and forskolin, and to the odorant mixture.

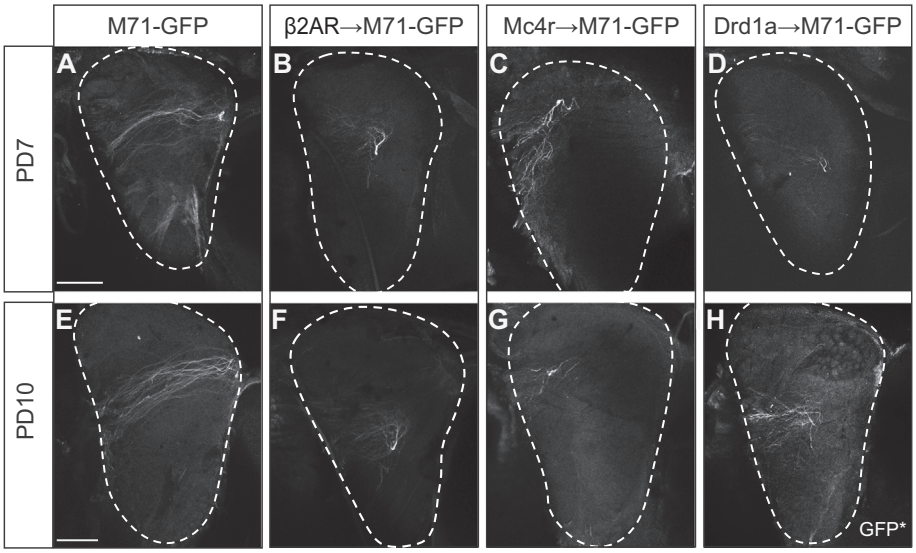

Fig. 6. Projections of OSN axons in Mc4r → M71-GFP and Drd1a → M71-GFP mice.
Intrinsic green fluorescence (GFP*) of medial views of wholemounts of olfactory bulbs of mice at PD7 (A–D) and PD10 (E–H). In M71-GFP mice, OSN axons coalesced and formed glomeruli at posterior-dorsal positions (A, E). In β2AR → M71-GFP mice, OSN axons coalesced and formed glomeruli at anterior-ventral positions (B,F). In Mc4r → M71-GFP mice, labeled axons coalesced at more anterior positions (C,G). In Drd1a → M71-GFP mice, labeled axons converged or fasciculated (D,H) at positions that are anterior and ventral to M71-GFP glomeruli and similar to β2AR → M71-GFP glomeruli. Scale bars: in A for A,B and in E for E–H, 500 μm. (For interpretation of the references to color in this figure legend, the reader is referred to the web version of this article.)

axons coalesced at more anterior positions (Fig. 6C) in comparison with labeled glomeruli in M71-GFP mice. In Drd1a → M71-GFP mice at PD7, labeled axons fasciculated and some of them converged (Fig. 6D) at positions similar to labeled glomeruli in β2AR → M71-GFP mice (Omura et al., 2014), and anterior and ventral to labeled glomeruli in M71-GFP mice. We also examined mice at PD10. Labeled glomeruli in M71-GFP mice had grown larger at PD10 (Fig. 6E). In Mc4r → M71-GFP mice at PD10, OSN axons coalesced at anterior-dorsal positions (Fig. 6G), as they did at PD7. In Drd1a → M71-GFP mice at PD10, we observed OSN axonal convergence or fasciculation (Fig. 6H) at positions that were anterior and posterior to labeled glomeruli in M71-GFP mice and similar to labeled glomeruli in β2AR → M71-GFP mice (Fig. 6F). Thus, Mc4r → M71-GFP OSN axons coalesced at more anterior and more dorsal positions compared to β2AR → M71-GFP OSN axons, and at more anterior positions compared to M71-GFP OSN axons; Drd1a → M71-GFP OSN axons fasciculated or converged at positions similar to β2AR → M71-GFP OSN axons.

Next we made coronal cryosections of olfactory bulbs of three M71-GFP mice, three β2AR → M71-GFP mice, seven Mc4r → M71-GFP mice, and five Drd1a → GFP mice at PD10. In Mc4r → M71-GFP mice, we found that four mice had one labeled glomerulus medially, one mouse had two labeled glomeruli medially, and two mice had no labeled glomerulus. We did not observe any labeled glomeruli laterally. Following a method that we described previously (Bressel et al., 2016), we estimated that the volume of Mc4r → M71-GFP glomeruli at PD10 is 20% of the volume of M71-GFP glomeruli, and 51% of the volume of β2AR → M71-GFP mice: 5726 ± 1963 μm^3 compared to 28,387 ± 8539 μm^3 and 11,112 ± 4300 μm^3 respectively (± STDV, $p < 0.005$ and $p < 0.05$, respectively, Student's *t*-test, n = 6). We did no find labeled glomeruli in cryosections of olfactory bulbs of five Drd1a → M71-GFP mice at PD10.

3.6. Mc4r glomeruli are innervated by VGLUT2+ and MAP2+ neurites

We observed immunoreactivity against Mc4r in GFP+ glomeruli in coronal cryosections of olfactory bulbs from Mc4r → M71-GFP mice at PD10 (Fig. 7A). In Drd1a → M71-GFP mice at PD10, we observed OSN axon fascicles that were immunoreactive for Drd1a and GFP, but no coalescence into glomeruli (Fig. 7B). We performed immunohistochemistry against GFP and vesicular glutamate receptor 2 (VGLUT2), a marker for presynaptic axonal terminals (Richard et al., 2010), and against microtubule-associated protein 2 (MAP2), a marker for postsynaptic dendrites (Kasowski et al., 1999). OSN axon termini within glomeruli were colabeled with GFP and VLGUT2 in M71-GFP mice (Fig. 7C) and in β2AR → M71-GFP mice (Fig. 7D). MAP2 immunoreactivity in M71-GFP mice (Fig. 7E) and in β2AR → M71-GFP mice (Fig. 7F) was detected within glomeruli in patterns that were complementary to GFP immunoreactivity. In Mc4r → M71-GFP mice, we found that GFP+ glomeruli were colabeled for VGLUT2 (Fig. 7G), and that MAP2+ immunoreactivity was complementary to GFP immunoreactivity within these glomeruli (Fig. 7H). In Drd1a → M71-GFP mice, we observed that GFP+ OSN axons fasciculated but did not coalesce; instead, they entered 3–5 glomeruli that were immunoreactive for VLUT2 and MAP2 (Fig. 7I, J).

3.7. OSN axonal projection patterns

Fig. 8 provides a schematic overview of the projections patterns of labeled OSN axons in the various strains. In wholemounts of olfactory bulbs of β2AR → M71-GFP mice at PD7 and PD10, we found medial GFP+ glomeruli in 5/6 olfactory bulbs. In Mc4r → M71-IRES-tauGFP mice, we found GFP+ glomeruli in 3/8 and 6/21 olfactory bulbs at PD7 and PD10, respectively. When labeled glomeruli were not apparent, we observed complex patterns of axons converging at anterior-dorsal positions in the olfactory bulb. In Drd1a → M71-GFP mice, 2/16 and 1/28 olfactory bulbs showed axonal convergence at PD7 and PD10, respectively. In Drd1a → M71-GFP mice, we found that OSN axons fasciculated in various conformations at anterior-ventral positions in 8/16 and 22/28 olfactory bulbs at at PD7 and PD10, respectively.

4. Discussion

Mouse ORs have very diverse functions in OSNs. First, the primary function of ORs is to serve as receptors for odorants. Expression in OSN dendritic cilia and coupling to Gnal (and Gnas) are prerequisites for ORs to bind odorants in the inhaled air and to transduce signals via cAMP in OSNs. Second, ORs are closely involved in regulating their own gene expression, such that a mature OSN typically expresses one allele of one OR gene. The tight control of expression of the largest gene repertoire in the genome appears to be regulated by having an OR that is expressed first and/or at high levels negatively control the expression of the rest of the repertoire. Third, OR proteins are also present in axons and axon terminals within glomeruli, and genetic experiments have indicated that ORs are closely involved in the coalescence of axons of OSNs that express the same OR into homogeneous glomeruli. Thus, OR fulfill at least three diverse functions in OSNs.

OSNs express normally a variety of other GPCRs (Sammeta et al., 2007) such as Drd2 (Ennis et al., 2001; Omura et al., 2014). Have ORs

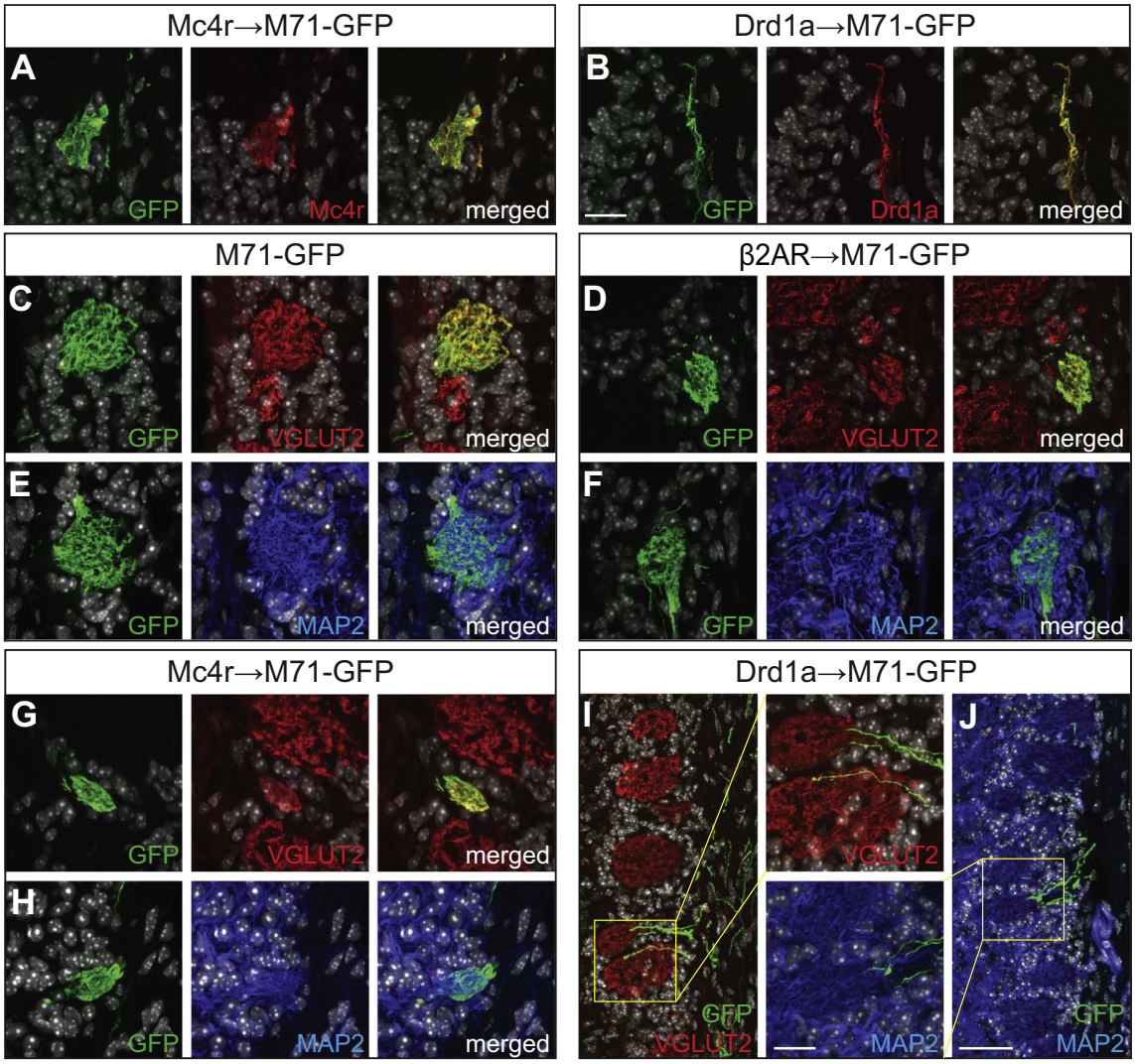

Fig. 7. Axons of Mc4r → M71-GFP OSNs form glomeruli, but axons of Drd1a → M71-GFP OSNs do not.
(A) Immunohistochemistry against GFP (green) and Mc4r (red) in a coronal cryosection of the olfactory bulb of a Mc4r → M71-GFP mouse at PD10. Labeled axons form a glomerulus.
(B) Immunohistochemistry against GFP and Drd1a in a coronal cryosection of the olfactory bulb of a Drd1a → M71-GFP mouse at PD10. Labeled axons form a fascicle.
(C–H) Immunohistochemistry against GFP (green), VGLUT2 (red), and MAP2 (blue) in a coronal cryosections of the olfactory bulbs of M71-GFP mice (C, E), β2AR → M71-GFP mice (D, F), and Mc4r → M71-GFP mice (G,H) at PD10.
(G1–H2) Labeled axons in a Drd1a → M71-GFP mouse at PD10 fasciculate and enter several glomeruli. Insets in the column between G and H represent higher magnifications.
Scale bars: in B for A-H, 20 μm; in J for I and J, 50 μm; in the bottom inset for the insets in the column between I and J, 20 μm. (For interpretation of the references to color in this figure legend, the reader is referred to the web version of this article.)

evolved special properties to serve these three diverse functions? Or is it merely the high-level expression of a GPCR from an OR locus that enables them to control expression of the OR gene repertoire and to mediate homotypic coalescence of OSN axons into homogeneous glomeruli?

4.1. β2AR can serve as surrogate OR in OSNs

An informative experimental approach over the past two decades has been to replace the coding region of OR x with that of OR y, in order to determine if the properties of OR x are now replaced by those of OR y

	β2AR→M71-GFP		Mc4r→M71-GFP		Drd1a→M71-GFP	
age	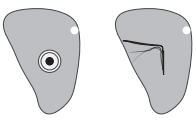		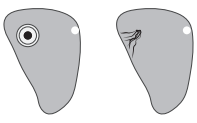		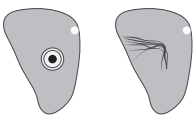	
PD7	5/6	1/6	3/8	5/8	2/16	8/16
PD10	5/6	1/6	6/21	12/21	1/28	22/28

Fig. 8. Patterns of OSN axonal projections in β2AR → M71-GFP, Mc4r → M71-GFP, and Drd1a → M71-GFP mice.
Schematic medial views of the olfactory bulb of mice at PD7 and PD10. White dots represent the area where M71-GFP glomeruli reside. Homocentric cycles represent areas where glomeruli reside in Mc4r → M71-GFP mice and where axons converge in Drd1a → M71-GFP mice. Black lines represent the most common patterns of axonal convergence or fasciculation in Mc4r → M71-GFP and Drd1a → M71-GFP mice, respectively.

(Mombaerts et al., 1996; Bozza et al., 2002; Feinstein and Mombaerts, 2004). A variant of this theme is to replace the coding region of an OR by that of a non-olfactory GPCR that is normally not expressed in OSNs and that is known to couple to Gnal and/or to Gnas. We (Feinstein et al., 2004; Omura et al., 2014) and others (Aoki et al., 2013; Nakashima et al., 2013) have shown that the β2-adrenergic receptor can serve very well as surrogate OR in OSNs. This surrogate function is studied optimally when β2AR is expressed from an endogenous OR locus by gene targeting in ES cells; we generated β2AR → M71-IRES-taulacZ mice (Feinstein et al., 2004) and β2AR → M71-IRES-tauGFP mice (Omura et al., 2014). We found that mouse β2AR can serve as surrogate OR in OSNs in terms of monoallelic and monogenic expression, subcellular localization, and responses to its agonist isoproterenol. Moreover, axons of β2AR → M71 coalesced into homogeneous glomeruli, at locations in the olfactory bulb that were anterior and ventral to those of the endogenous M71 glomeruli. Thus, for all properties that we examined, we found that β2AR can serve as surrogate OR in OSNs. Others generated transgenic strains in which wild-type or mutant β2AR was expressed from a transgenic MOR23 promoter (Aoki et al., 2013; Nakashima et al., 2013).

4.2. Mc4r and Drd1a can serve partially as surrogate ORs in OSNs

Can other non-olfactory GPCRs serve also as surrogate ORs in OSNs? To enable comparison with our results from the β2AR → M71 strains and to cope with the well-known variability of transgenic strains, we expressed two other non-olfactory mouse GPCRs from the *M71* locus by gene targeting. We followed four criteria to narrow down our choice to Mc4r and Drd1a. First, these non-olfactory GPCRs are normally not expressed in OSNs. Second, as it the case for OR genes, their coding region consists of a single coding exon, avoiding possible complications from alternatively spliced transcripts. Third, they couple to Gnal and/or Gnas. Fourth, selective agonists are commercially available. Moreover, we opted for GPCRs about which much is known, paving the way to test functionality of mutant versions of the non-olfactory GPCR in future studies.

Mc4r is one of five melanocortin receptors and is involved in regulating energy homeostasis. Recessive mutations in the human *MC4R* gene are the most common monogenic form of morbid obesity (Tao, 2010). This GPCR has several endogenous agonists that are formed by processing of the *Pomc* gene, and, interestingly, it has also endogenous antagonists, agouti and agouti-related protein (also an inverse agonist). Mc4r possess unique sequence features in comparison with other Class A GPCRs and ORs; for instance, the highly-conserved motif NPxIY found in Class A GPCRs has an aspartic acid (D) instead of an asparagine (N) in Mc4r. Drd1a is one of five dopamine receptors, among which only Drd2 is expressed in OSNs (Sammeta et al., 2007; Omura et al., 2014). In the striatum Drd1a signaling involves binding to Gnal (Zhuang et al., 2000). We found that both non-olfactory GPCRs can substitute for M71, but not as efficiently as β2AR. The number of OSNs expressing these non-olfactory GPCRs from the *M71* locus is reduced by a factor of three-fold, as is the case with β2AR → M71-GFP.

Axons from Mc4r → M71-GFP OSNs form, in some cases, glomeruli. The positions of these glomeruli are more anterior than those of the endogenous M71 glomeruli, and also different from those of β2AR → M71-GFP glomeruli. Axons from Drd1a → M71-GFP OSNs have great difficulty forming glomeruli. Nonetheless they fasciculate, which is consistent with homotypic interactions (Feinstein and Mombaerts, 2004), and some axons appear to converge. We attribute the weak performance of Drd1a → M71-GFP to the poor maturation of the OSNs: only 6% of the 1000 OSNs (a mere 60 cells) expressing this allele are fully mature (*Omp* + *Gap43*-). This number may be far below the minimum to form and maintain glomeruli (Ebrahimi and Chess, 2000). We have no plausible explanation why Drd1a → M71-GFP OSNs mature with such difficulty. One possibility is that dopamine chronically stimulates these OSNs, thereby hampering their maturation or survival. The decreased efficiency of Mc4r as a surrogate OR compared to β2AR could be related to several differences between the amino acid sequences of Mc4r and ORs. But in the absence of functional data, it would be speculative to attribute the lower efficiency to one or more of these differences in amino acid residues.

Nevertheless, we have now shown that three out of three non-olfactory GPCRs, with varying characteristics and ligands, can serve, partially or fully, as surrogate OR in OSNs when expressed from the *M71* locus. Thus, there appear to be no features or properties that are unique or specific to ORs with regard to their functions in odorant reception, OR gene choice, and OSN axonal coalescence into glomeruli.

5. A look ahead

Among 11 OR genes that we surveyed, we found a 17-fold range in the numbers of OSNs per mouse that express a given OR gene (Bressel et al., 2016). *M71* was the last-but-lowest expressed OR gene in this study. A greater number of mature OSNs expressing a GCPR → OR allele could be obtained by expressing a non-olfactory GPCR from an OR locus with a greater probability of choice, such as the *MOR256-17/Olfr15* locus (Bressel et al., 2016). Olfr15 is well characterized and confers extremely broad responsiveness to odorants in OSNs (Tazir et al., 2016). OSN maturation may be improved by mutations that increase the constitutive activity of the non-olfactory GPCR, such as those described functionally for Mc4r or protecting phenotypically against obesity in humans (Tao, 2010). The electrophysiological responses to cognate agonists that we have described here in Mc4r → M71-GFP and Drd1a → M71-GFP OSNs could be employed to develop in vivo or ex vivo screening strategies for molecules with agonist, antagonist, or inverse agonist activity.

Acknowledgments

P.M. is grateful to the Max Planck Society for generous financial support. The work of X.G. was supported by the CNRS and the Conseil Régional de Bourgogne.

References

Agosti, F., López Soto, E.J., Cabral, A., Castrogiovanni, D., Schioth, H.B., Perelló, M., Raingo, J., 2014. Melanocortin 4 receptor activation inhibits presynaptic N-type calcium channels in amygdaloid complex neurons. Eur. J. Neurosci. 40, 2755–2765.
Aoki, M., Takeuchi, H., Nakashima, A., Nishizumi, H., Sakano, H., 2013. Possible roles of Robo1+ ensheathing cells in guiding dorsal-zone olfactory sensory neurons in mouse. Dev. Neurobiol. 73, 828–840.
Barnea, G., O'Donnell, S., Mancia, F., Sun, X., Nemes, A., Mendelsohn, M., Axel, R., 2004. Odorant receptors on axon termini in the brain. Science 304, 1468.
Beaulieu, J.-M., Gainetdinov, R.R., 2011. The physiology, signaling, and pharmacology of dopamine receptors. Pharmacol. Rev. 63, 182–217.
Belluscio, L., Gold, G.H., Nemes, A., Axel, R., 1998. Mice deficient in G_{olf} are anosmic. Neuron 20, 69–81.
Benoit, S.C., Schwartz, M.W., Lachey, J.L., Hagan, M.M., Rushing, P.A., Blake, K.A., Yagaloff, K.A., Kurylko, G., Franco, L., Danhoo, W., Seeley, R.J., 2000. A novel selective melanocortin-4 receptor agonist reduces food intake in rats and mice without producing aversive consequences. J. Neurosci. 20, 3442–3448.
Bozza, T., Feinstein, P., Zheng, C., Mombaerts, P., 2002. Odorant receptor expression defines functional units in the mouse olfactory system. J. Neurosci. 22, 3033–3043.
Bressel, O.C., Khan, M., Mombaerts, P., 2016. Linear correlation between the number of olfactory sensory neurons expressing a given mouse odorant receptor gene and the total volume of the corresponding glomeruli in the olfactory bulb. J. Comp. Neurol. 524, 199–209.
Buck, L., Axel, R., 1991. A novel multigene family may encode odorant receptors: a molecular basis for odor recognition. Cell 65, 175–187.
Chess, A., Simon, I., Cedar, H., Axel, R., 1994. Allelic inactivation regulates olfactory receptor gene expression. Cell 78, 823–834.
Dietschi, Q., Assens, A., Challet, L., Carleton, A., Rodriguez, I., 2013. Convergence of FPR-rs3-expressing neurons in the mouse accessory olfactory bulb. Mol. Cell. Neurosci. 56, 140–147.
Ennis, M., Zhou, F.M., Ciombor, K.J., Aroniadou-Anderjaska, V., Hayar, A., Borrelli, E., Zimmer, L.A., Margolis, F., Shipley, M.T., 2001. Dopamine D2 receptor-mediated presynaptic inhibition of olfactory nerve terminals. J. Neurophysiol. 86, 2986–2997.
Ebrahimi, F.A., Chess, A., 2000. Olfactory neurons are interdependent in maintaining axonal projections. Curr. Biol. 10, 219–222.
Feinstein, P., Bozza, T., Rodriguez, I., Vassalli, A., Mombaerts, P., 2004. Axon guidance of

mouse olfactory sensory neurons by odorant receptors and the β2 adrenergic receptor. Cell 117, 833–846.
Feinstein, P., Mombaerts, P., 2004. A contextual model for axonal sorting into glomeruli in the mouse olfactory system. Cell 117, 817–831.
Gantz, I., Miwa, H., Konda, Y., Shimoto, Y., Tashiro, T., Watson, S.J., DelValle, J., Yamada, T., 1993. Molecular cloning, expression, and gene localization of a fourth melanocortin receptor. J. Biol. Chem. 268, 15174–15179.
Giuliani, D., Mioni, C., Bazzani, C., Zaffe, D., Botticelli, A.R., Capolongo, S., Sabba, A., Galantucci, M., Iannone, A., Grieco, P., Novellino, E., Colombo, G., Tomasi, A., Catania, A., Guarini, S., 2007. Selective melanocortin MC4 receptor agonists reverse haemorrhagic shock and prevent multiple organ damage. Br. J. Pharmacol. 150, 595–603.
Grosmaitre, X., Fuss, S.H., Lee, A.C., Adipietro, K.A., Matsunami, H., Mombaerts, P., Ma, M., 2009. SR1, a mouse odorant receptor with an unusually broad response profile. J. Neurosci. 29, 14545–14552.
Grosmaitre, X., Vassalli, A., Mombaerts, P., Shepherd, G.M., Ma, M., 2006. Odorant responses of olfactory sensory neurons expressing the odorant receptor MOR23: a patch clamp analysis in gene-targeted mice. Proc. Natl. Acad. Sci. U. S. A. 103, 1970–1975.
Ishii, T., Omura, M., Mombaerts, P., 2004. Protocols for two- and three-color fluorescent RNA in situ hybridization of the main and accessory olfactory epithelia in mouse. J. Neurocytol. 33, 657–669.
Jones, D.T., Reed, R.R., 1989. G_{olf}: an olfactory neuron specific-G protein involved in odorant signal transduction. Science 22, 790–795.
Kasowski, H.J., Kim, H., Greer, C.A., 1999. Compartmental organization of the olfactory bulb glomerulus. J. Comp. Neurol. 407, 261–274.
Lam, R., Mombaerts, P., 2013. Odorant responsiveness of embryonic mouse olfactory sensory neurons expressing the odorant receptors S1 or MOR23. Eur. J. Neurosci. 38, 2210–2217.
Li, J., Ishii, T., Feinstein, P., Mombaerts, P., 2004. Odorant receptor gene choice is reset by nuclear transfer from mouse olfactory sensory neurons. Nature 428, 393–399.
Ma, M., Chen, W.R., Shepherd, G.M., 1999. Electrophysiological characterization of rat and mouse olfactory receptor neurons from an intact epithelial preparation. J. Neurosci. Methods 92, 31–40.
Malnic, B., Hirono, J., Sato, T., Buck, L.B., 1999. Combinatorial receptor codes for odors. Cell 96, 713–723.
Mombaerts, P., Wang, F., Dulac, C., Chao, S.K., Nemes, A., Mendelsohn, M., Edmondson, J., Axel, R., 1996. Visualizing an olfactory sensory map. Cell 87, 675–686.
Nakashima, A., Takeuchi, H., Imai, T., Saito, H., Kiyonari, H., Abe, T., Chen, M., Weinstein, L.S., Yu, C.R., Storm, D.R., et al., 2013. Agonist-independent GPCR activity regulates anterior-posterior targeting of olfactory sensory neurons. Cell 154, 1314–1325.
Neumeyer, J.L., Kula, N.S., Bergman, J., Baldessarini, R.J., 2003. Receptor affinities of dopamine D1 receptor-selective novel phenylbenzazepines. Eur. J. Pharmacol. 474, 137–140.
Omura, M., Grosmaitre, X., Ma, M., Mombaerts, P., 2014. The β2-adrenergic receptor as a surrogate odorant receptor in mouse olfactory sensory neurons. Mol. Cell. Neurosci. 58, 1–10.
Rashid, A.J., So, C.H., Kong, M.M.C., Furtak, T., El-Ghundi, M., Cheng, R., O'Dowd, B.F., George, S.R., 2007. D1-D2 dopamine receptor heterooligomers with unique pharmacology are coupled to rapid activation of Gq/11 in the striatum. Proc. Natl. Acad. Sci. U. S. A. 104, 654–659.
Richard, M.B., Taylor, S.R., Greer, C.A., 2010. Age-induced disruption of selective olfactory bulb synaptic circuits. Proc. Natl. Acad. Sci. U. S. A. 107, 15613–15618.
Sammeta, N., Yu, T.T., Bose, S.C., McClintock, T.S., 2007. Mouse olfactory sensory neurons express 10,000 genes. J. Comp. Neurol. 502, 1138–1156.
Strotmann, J., Conzelmann, S., Beck, A., Feinstein, P., Breer, H., Mombaerts, P., 2000. Local permutations in the glomerular array of the mouse olfactory bulb. J. Neurosci. 20, 6927–6938.
Strotmann, J., Levai, O., Fleischer, J., Schwarzenbacher, K., Breer, H., 2004. Olfactory receptor proteins in axonal processes of chemosensory neurons. J. Neurosci. 24, 7754–7761.
Tao, Y.X., 2010. The melanocortin-4 receptor: physiology, pharmacology, and pathophysiology. Endocr. Rev. 31, 506–543.
Tazir, B., Khan, M., Mombaerts, P., Grosmaitre, X., 2016. The extremely broad odorant response profile of mouse olfactory sensory neurons expressing the odorant receptor MOR256-17 includes trace amine-associated receptor ligands. Eur. J. Neurosci. 43, 608–617.
Vassalli, A., Rothman, A., Feinstein, P., Zapotocky, M., Mombaerts, P., 2002. Minigenes impart odorant receptor-specific axon guidance in the olfactory bulb. Neuron 35, 681–696.
Zapiec, B., Mombaerts, P., 2015. Multiplex assessment of the positions of odorant receptor-specific glomeruli in the mouse olfactory bulb by serial two-photon tomography. Proc. Natl. Acad. Sci. U. S. A. 112, E5873–5882.
Zhuang, X., Belluscio, L., Hen, R., 2000. $G_{OLF\alpha}$ mediates dopamine D1 receptor signaling. J. Neurosci. 20, RC91 (1–5).